Sainmatika: Jurnal Ilmiah Matematika dan Ilmu Pengetahuan Alam
Volume 22 No. 2, December 2025 DOI 10.31851/sainmatika.v22i2.20191
https://jurnal.univpgri-palembang.ac.id/index.php/sainmatika

# Reusability and Reaction Kinetics of Pillared Palm Shell-Based Activated Carbon for Synthetic Dye Adsorption

Dian Sari Dewi, Surya Hatina, Risqi Saputra, Sisnayati, Dewi Putri Yuniarti, Ria Komala*
*e-mail: ria.komala0411@gmail.com

*Department of Chemical Engineering, Faculty of Engineering, Universitas Tamansiswa Palembang, Indonesia*

## ABSTRACT

The increasing discharge of synthetic dye effluents from industrial processes poses severe environmental concerns due to their toxicity, persistence, and aesthetic impact on water bodies. This study investigates the reusability potential and reaction kinetics of aluminum/iron-pillared activated carbon derived from palm shell biomass for synthetic dye adsorption. Activated carbon was prepared through carbonization, acid activation, and metal pillaring, followed by multiple adsorption–desorption cycles using a 25 ppm dye solution. Adsorption efficiency was evaluated over five consecutive reuse cycles, while kinetic models including zero-, first-, and second-order reactions were applied to elucidate the adsorption mechanism. Fourier Transform Infrared (FTIR) analysis revealed the presence of functional groups such as hydroxyl, carbonyl, and amine groups, indicating enhanced surface activity after metal pillaring. Results showed that adsorption efficiency peaked at the fourth cycle with a 76.67% color removal before declining due to pore saturation and fouling effects. Kinetic analysis demonstrated that the adsorption process followed a zero-order reaction model ($R^2$ = 0.878), suggesting constant adsorption rates independent of dye concentration. These findings highlight the feasibility of reusing pillared palm shell-based activated carbon for wastewater treatment applications and provide insights into its regeneration strategies for sustainable pollutant removal.

**Keywords**: Palm shell, pillared activated carbon, adsorption, reusability, adsorption kinetics

## INTRODUCTION

Biomass-based activated carbon has been widely used as an effective adsorbent for the removal of color from industrial wastewater due to its high porosity, large surface area, and excellent chemical and thermal stability. One promising source of biomass is palm shell, a by-product of the palm oil industry, which is commonly utilized only as boiler fuel. Processing palm shells into aluminum/iron (Al/Fe)-pillared activated carbon has been reported to enhance adsorption capacity and material stability, thereby improving its effectiveness in removing dyes from wastewater (Ullah et al., 2024)

In industrial practice, the reuse of activated carbon is an important strategy to reduce operational costs. However, repeated use can decrease adsorption efficiency due to active site saturation, pore fouling, and structural degradation of the carbon (Baskar et al., 2022a). Therefore, evaluating adsorption efficiency across multiple reuse cycles and understanding the reaction kinetics are essential to determine service life, regeneration strategies, and to maintain adsorbent performance. Based on this need, the research question arises as to how repeated use of Al/Fe-pillared palm shell activated carbon affects the efficiency of color removal from wastewater and which adsorption kinetic model best explains the rate of color removal over multiple reuse cycles.

*p-ISSN 1829 586X*
*e-ISSN 2581-0170*

Although several studies have investigated the use of biomass-based activated carbon and metal-pillared activated carbon for dye removal, examples include research on Direct Yellow 12 adsorption using biomass-based activated carbon with isotherm and kinetic modeling (Reddy et al., 2025). studies on microporous activated carbon derived from biomass waste with KOH activation for methylene blue adsorption and surface mechanistic analysis (Jawad et al., 2021). as well as research on improved textile dye adsorption using sulfonated activated carbon derived from pomegranate peel waste (Thamer et al., 2023). However, studies specifically evaluating adsorption efficiency during multiple reuse cycles, particularly for Al/Fe-pillared palm shell activated carbon, remain limited. Most previous research has focused more on physicochemical characterization of the adsorbent rather than systematically linking reuse data with adsorption reaction kinetics.

This study therefore addresses the research gap by combining adsorption efficiency evaluation over multiple reuse cycles with kinetic analysis of dye adsorption using Al/Fe-pillared palm shell activated carbon. In this process, aluminum and iron hydroxide species ($Al(OH)_3$ and $Fe(OH)_3$) are intercalated between the carbon layers, forming stable pillars that increase the surface area, pore volume, and thermal stability of the adsorbent. These pillars provide abundant active sites that enhance electrostatic attraction and chemical bonding with dye molecules during adsorption. The adsorption mechanism of Al/Fe-pillared activated carbon, illustrated schematically in Figure 1, involves ion exchange between $Al^{3+}$/$Fe^{3+}$ and surface functional groups, followed by dye molecule capture within the developed micropores and mesopores. This approach enables the identification of the initial, optimal, and declining phases of adsorption efficiency caused by adsorbent saturation, while determining the most suitable kinetic model.

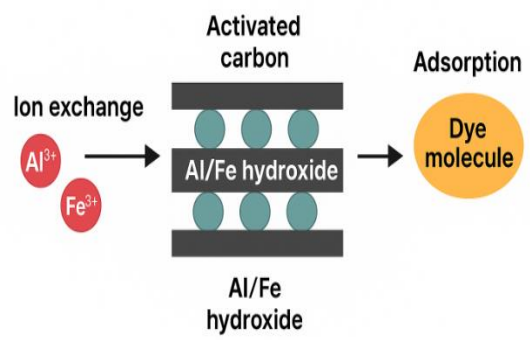


Figure 1. Adsorption mechanism using Al/Fe- pillared active carbon.

The objectives of this research are to assess the adsorption efficiency of Al/Fe-pillared palm shell activated carbon across multiple reuse cycles and to determine the adsorption reaction kinetics, thereby providing insights into the rate and mechanism of dye removal and supporting the optimization of adsorbent use in industrial applications.

## MATERIALS AND METHODS

### Materials

The main material used in this study was palm shell obtained from a palm oil mill located at Dermaga Pelabuhan Dalam, Tanjung Api-Api, Banyuasin Regency, South Sumatra, Indonesia. The chemicals used included 5% $H_2SO_4$ solution as the activating agent, and $Al(NO_3)_3 \cdot 9H_2O$ and $Fe(NO_3)_3 \cdot 9H_2O$ (0.5 M) as the pillaring agents. A Dylon (Hb09) dye solution with a concentration of 25 ppm was used as the test solution for adsorption experiments. The equipment employed included a drying oven (WTC Binder muffle furnace, Thermo Scientific Thermolyne F48050-33), furnace, UV-Vis spectrophotometer (Shimadzu UV-1800), pH meter (Hanna HI-2211), analytical balance (Ohaus Pioneer

PA214), and standard laboratory glassware.

## Methods

### Preparation of Metal-Pillared Activated Carbon

Palm shells were cleaned, dried, and cut into pieces of approximately 5 mm. Carbonization was carried out at 400°C for 2 hours to produce char. The resulting char was then activated using 200 mL of 5% $H_2SO_4$ solution, followed by pillaring with a mixture of $Al(OH)_3$ and $Fe(OH)_3$. The pillared material was subsequently calcined at 400°C for 2 hours before being analyzed.

### Repeated Adsorption Process

The Al/Fe-pillared activated carbon obtained was used for repeated adsorption experiments with a 25 ppm dye solution. In each cycle, 2 grams of activated carbon were mixed with the dye solution and stirred at 200 rpm for 120 minutes to ensure uniform contact between the adsorbent and the dye molecules. After each adsorption process, the mixture was filtered, and the residual dye concentration was measured using a UV–Vis spectrophotometer (Shimadzu UV-1800) at a wavelength of 546 nm**,** corresponding to the maximum absorbance of the Dylon (Hb09) dye. A standard calibration curve was prepared from dye concentrations ranging from 5 ppm to 50 ppm to determine the residual concentration accurately. The adsorption process was repeated for up to five cycles to evaluate the adsorption efficiency during repeated use.

### Data Analysis

The adsorption efficiency (E, %**)** was calculated based on the difference between the initial and final dye concentrations for each cycle, as expressed in Equation (1):

$$E(\%) = \frac{C_0 - C_t}{C_0}\ x\ 100 \qquad (1)$$

where $C_o$ and Ct (mg/L) are the initial and residual dye concentrations, respectively, measured using a UV–Vis spectrophotometer (Shimadzu UV-1800) at 546 nm.

The kinetic data obtained from the adsorption experiments were analyzed using three kinetic models: zero-order, first-order, and second-order, as given in Equations (2) – (4):

**Zero-Order:**

$$[A] = [A]_0 - kt \qquad (2)$$

**First-Order:**

$$ln[A] = ln[A]_0 - kt \qquad (3)$$

**Second-Order:**

$$\frac{1}{[A]} = \frac{1}{[A]_0} + kt \qquad (4)$$

The kinetic model with the highest determination coefficient ($R^2$) was identified as the most appropriate to describe the adsorption mechanism. The data obtained from repeated adsorption experiments were also used to evaluate the potential reusability of the spent activated carbon prior to regeneration or its utilization as a raw material for energy briquette production.

## RESULTS AND DISCUSSION

### Characteristics of Palm Shell Activated Carbon

FTIR (Fourier Transform Infrared Spectroscopy) is a commonly used method to identify functional groups on the surface of materials, including activated carbon. (Dittmann et al., 2022). In this study, the activated carbon used was derived from palm shells that had been metal-pillared, specifically prepared to enhance the adsorption capacity toward synthetic dye compounds. The analyzed samples represented activated carbon before and after the adsorption process. By comparing the spectra of both samples, the changes occurring on the activated carbon surface after

interaction with dye molecules can be better understood.

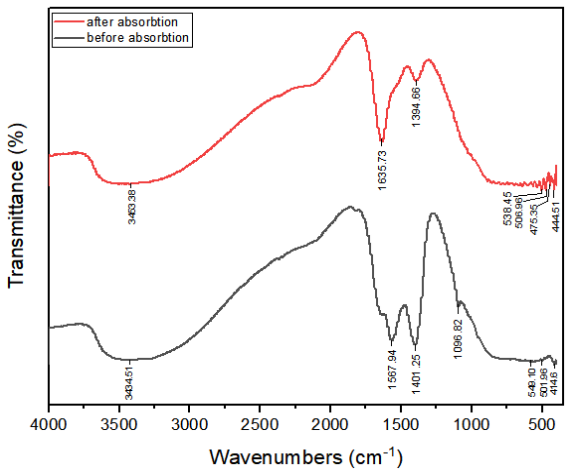


Figure 1. FTIR spectra of metal-pillared activated carbon before and after adsorption

Based on the FTIR data from the two samples, the following discussion presents the analysis results and their implications for the adsorption process of synthetic dye wastewater:

**FTIR Spectrum Analysis Before Adsorption.**

The FTIR spectrum of the metal-pillared palm shell activated carbon before adsorption showed several characteristic peaks associated with active functional groups on the surface. The peak at 1096.82 $cm^{-1}$ was attributed to C–O or possibly Si–O stretching vibrations, indicating the involvement of metal pillars (Al/Fe) in the activated carbon structure. The presence of these metal pillars has been reported to increase the surface area and introduce additional active sites for the adsorption process, as demonstrated by Mechnou et al. (2025), who showed that metal modification of carbon surfaces enhances affinity toward polar organic compounds. (Mechnou et al., 2025).

Furthermore, the peak at 1401.25 $cm^{-1}$ was associated with the vibration of carbonyl (C=O) groups originating from the oxidation of the carbon surface. The presence of these oxygen-containing groups is important because it enhances the hydrophilic properties and facilitates electrostatic interactions with charged dye molecules. As reported by Rizwan et al. (2020), oxygen functional groups on the carbon surface play a significant role in improving the adsorption capacity for synthetic dyes (Ali et al., 2020).

Another peak at 1567.94 $cm^{-1}$ was attributed to the vibrations of amine or amide groups (N–H/C=N), which also play an important role in the formation of hydrogen bonds or electrostatic interactions between the carbon surface and dye molecules. Recent studies have reported that nitrogen-enriched activated carbon derived from biomass, including the presence of nitrogen functional groups, significantly influences the adsorption properties. (Bumajdad et al., 2023)

Overall, the FTIR spectrum indicates that the metal-pillared palm shell activated carbon possesses oxygen- and nitrogen-containing functional groups that are ready to interact with dye molecules, supporting the adsorption process through both physical and chemical mechanisms. The relatively low intensity of peaks below 1000 $cm^{-1}$ also suggests that there are still surface areas that have not been fully modified, allowing for a potential increase in adsorption capacity with further pillaring treatment.

**FTIR Spectrum Analysis After Adsorption**

After the adsorption process, the FTIR spectrum showed significant changes. The peak at 1394.66 $cm^{-1}$ indicated strong interactions between the functional groups of the activated carbon and the dye molecules, potentially through hydrogen bonding or dipole interactions.

The peak at 1635.73 $cm^{-1}$ exhibited increased intensity, suggesting the adsorption of dye molecules, which may originate from C=C bonds in aromatic structures or N–H bonds from amide groups.

A decrease in intensity at the lower wavenumber peaks **(**416.83 $cm^{-1}$ to 538.45 $cm^{-1}$**)** revealed that the active sites previously available were utilized for dye adsorption, indicating the effectiveness of the activated carbon in interacting with and utilizing its adsorption capacity.

Overall, the FTIR analysis demonstrated that palm shell activated carbon was effective in adsorbing synthetic dye wastewater, as evidenced by the significant spectral changes observed after the adsorption process. (Alharbi et al., 2022).

## Repeated Use of Pillared Palm Shell Activated Carbon in the Adsorption Process

Table 1. Results of color analysis for the repeated use of pillared palm shell activated carbon as an adsorbent.

| Repeated Use | Color (TCU) | Color Removal Percentage (%) |
|---|---|---|
| 0 | 180 | - |
| 1 | 184 | (2.22) |
| 2 | 107 | 40.56 |
| 3 | 67 | 62.78 |
| 4 | 42 | 76.67 |
| 5 | 56 | 68.89 |

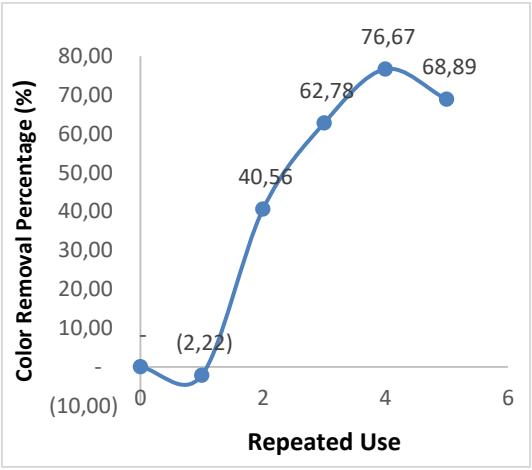


**Figure 2.** Graph of the effect of repeated adsorbent use on color degradation

Figure 2 shows the percentage of color degradation relative to the number of adsorption cycles using Al/Fe-pillared palm shell activated carbon. In the first cycle, color degradation showed a negative value (-2.22%). This is likely due to the initial desorption of dye molecules from the adsorbent surface, which was not yet fully stabilized. At this early stage, the active sites on the adsorbent may not have been completely available for interaction with the dye molecules. According to Le et al. (2024), desorption can occur due to an initial imbalance between the dye molecule concentration in the solution and the stability of the adsorbent surface (Le et al., 2024).

After the initial stage, color degradation increased significantly with the number of adsorption cycles, rising from 40.56% in the second cycle to a peak of 76.67% in the fourth cycle. This increase indicates optimal adsorption efficiency, where the active sites on the metal-pillared activated carbon began to be effectively utilized. The pillaring process with Al/Fe metals is known to enhance the adsorbent's surface area through the development of micro- and mesopores, while also strengthening the chemical and thermal stability of the adsorbent material. This finding aligns

with Peres et al. (2024), who reported that biomass-based activated carbon with metal pillaring exhibits a high surface area (up to 800 $m^2/g$) and optimal adsorption capacity at dye concentrations of 20–50 ppm. (Peres et al., 2024). *Akhtar et al. (2024)* also stated that the structure of the pillared adsorbent allows for increased adsorption efficiency due to the easier access of target molecules to the active sites (Akhtar et al., 2024).

However, after the fourth cycle, the adsorption efficiency decreased to 68.89%. This reduction can be attributed not only to the saturation of active sites, where most of the pores and surfaces of the adsorbent were already occupied by dye molecules, but also to partial desorption of previously adsorbed dyes. The weakening of physical interactions, such as van der Waals forces and hydrogen bonding between dye molecules and the adsorbent surface may cause the release of some adsorbed species during subsequent adsorption cycles.

Furthermore, the functional groups present on the Al/Fe-pillared activated carbon, such as hydroxyl (–OH), carboxyl (–COOH), and metal oxygen (M–O–Fe/Al) bonds, play a crucial role in chemical adsorption. These groups form electrostatic attractions and coordination bonds with dye molecules, contributing to both physisorption and chemisorption mechanisms. Over multiple cycles, partial deactivation or structural alteration of these active groups may occur, leading to reduced adsorption strength and selectivity.

In addition, fouling and pore blockage may result from the accumulation of non-desorbed dye molecules, thereby decreasing the accessible surface area and pore volume. Similar observations were reported by Kordijazi et al. (2021), who noted a 10–15% decline in efficiency of Al/Fe-based adsorbents after several reuse cycles due to pore clogging and contaminant buildup (Kordijazi, 2021). Meanwhile, Baskar et al. (2023) emphasized that adsorbent regeneration through thermal or chemical treatment after 4–5 cycles of use is essential to restore optimal performance and maintain surface activity (Baskar et al., 2022b).

Overall, the graph indicates three phases in the adsorption process: an initial phase where early desorption occurs, a growth phase with a significant increase in efficiency, and a decline phase due to adsorbent saturation. The literature supports these findings and provides additional insights into the need for adsorbent regeneration to maintain its efficiency in repeated applications. Regeneration strategies can serve as a solution to prevent fouling and extend the adsorbent's lifespan, enabling the adsorption process to operate more efficiently and economically.

**Reaction Kinetics**

In this analysis, absorbance data were used as an indicator of reactant concentration to determine the most appropriate kinetic model. By plotting absorbance versus time, as well as its logarithmic transformation (ln) and reciprocal (1/[A]), the linearity of the data could be evaluated to identify the reaction order, while also providing insights into the reaction mechanism and the factors influencing its rate.

The following presents the results of the reaction kinetics analysis based on the absorbance measurement data:

**1. Zero-Order Reaction**

A zero-order reaction represents a linear change in concentration over time. The reaction is described by Equation (1). The absorbance values for each contact time are presented in Table 2.

Table 2. Data on changes in absorbance with respect to contact time

| Contact Time and (min) | Absorbance |
|---|---|
| 0 | 0.363 |
| 30 | 0.359 |
| 60 | 0.338 |
| 90 | 0.310 |
| 120 | 0.251 |
| 150 | 0.135 |
| 180 | 0.157 |

The absorbance values decreased steadily from 0 to 150 minutes, indicating that dye molecules were actively adsorbed onto the surface of the Al/Fe-pillared activated carbon. This continuous decline shows that the adsorption process progressed efficiently as the available active sites and pores interacted with dye molecules in the solution.

However, a slight increase in absorbance was observed at 180 minutes. This phenomenon may be attributed to the desorption of dye molecules that were weakly bound to the adsorbent surface once the adsorption–desorption equilibrium was reached. After most active sites became saturated, the system may have undergone surface rearrangement or competitive displacement among dye molecules, leading to the release of a small portion of adsorbed dye back into the solution.

Similar behavior has been reported in other adsorption systems, where extended contact time beyond equilibrium causes partial desorption due to weakening of physical forces such as van der Waals and hydrogen bonding. Therefore, the optimum contact time for maximum dye removal was determined to be 150 minutes, beyond which further contact did not improve the adsorption efficiency.

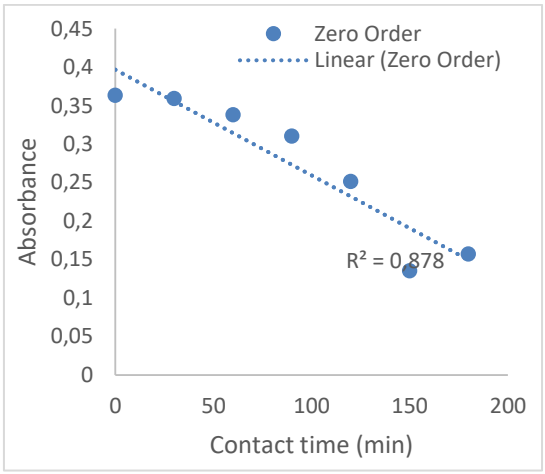


Figure 3. Contact Time vs. Absorbance for Zero-Order Reaction

Based on the reaction kinetics analysis, Figure 3, which shows the relationship between absorbance and time, indicates that the reaction tends to follow zero-order kinetics. The zero-order plot of absorbance versus time shows a linear decrease, with a determination coefficient ($R^2$) of 0.878. This suggests that the data fit the zero-order model well. In a zero-order reaction, the reaction rate does not depend on the reactant concentration but is influenced by external factors such as the presence of a catalyst. The reaction proceeds at a constant rate over time, consistent with the linear trend observed in the graph.

**2. First-Order Reaction**

A first-order reaction represents an exponential change in concentration. The reaction equation is shown in Equation (2). The ln(absorbance) data are presented in Table 3**.**

Table 3. Data on the relationship between contact time and ln(absorbance)

| Contact time (min) | Ln Absorbance |
|---|---|
| 0 | -1.013 |
| 30 | -1.024 |
| 60 | -1.085 |
| 90 | -1.171 |
| 120 | -1.382 |
| 150 | -2.002 |
| 180 | -1.852 |

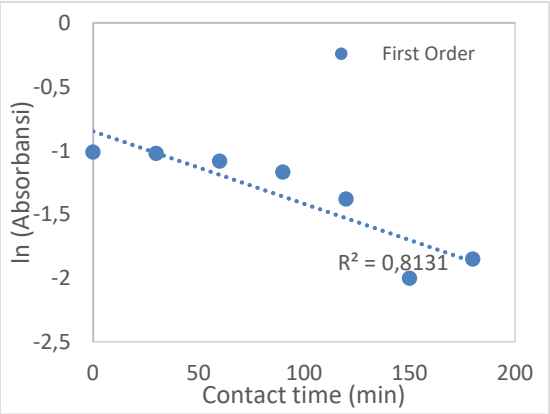


Figure 4. Contact Time vs. Absorbance for First-Order Reaction

Figure 4 shows the first-order reaction plot, which graphs the natural logarithm of absorbance (ln(absorbance)) versus time. The determination coefficient ($R^2$) is 0.813. Although this plot shows a relationship that is nearly linear, the $R^2$ value is lower compared to the zero-order model, indicating that the data fit the first-order kinetic model less accurately. In a first-order reaction, the reaction rate directly depends on the reactant concentration; however, this analysis suggests that the reaction does not fully follow this pattern.

### 3. Second-Order Reaction

A second-order reaction represents the relationship between time and the reciprocal of the concentration. The reaction equation is shown in Equation (3). The data for 1/absorbance at varying contact times are presented in Table 4.

Table 4. Data on 1/absorbance at different contact times

| Contact times (min) | 1/ Absorbance |
|---|---|
| 0 | 2.755 |
| 30 | 2.786 |
| 60 | 2.959 |
| 90 | 3.226 |
| 120 | 3.984 |
| 150 | 7.407 |
| 180 | 6.369 |

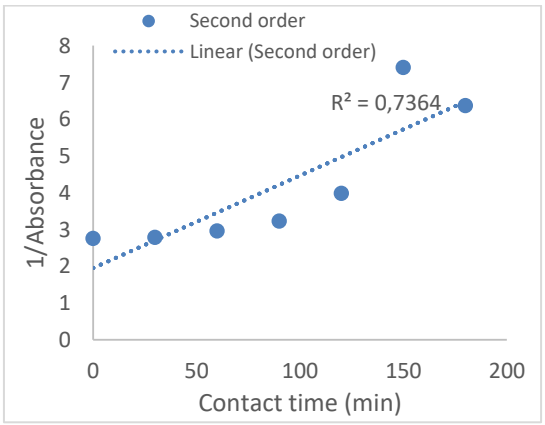


Figure 5. Contact Time vs. Absorbance for Second-Order Reaction

Figure 5 shows the second-order reaction plot, which graphs the reciprocal of absorbance (1/Absorbance) versus time. The determination coefficient ($R^2$) was 0.736, the lowest among the three models, indicating that the data fit the second-order kinetics model the least. In a second-order reaction, the reaction rate typically depends on the product of the concentrations of two reactants, which does not align with the observed pattern of absorbance reduction in this dataset.

Overall, the analysis results indicate that the reaction follows zero-order kinetics, where the reaction rate is independent of the reactant concentration.

The zero-order model provided the best fit to the data, with the highest linearity among the three models tested.

.

## CONCLUSION

This study demonstrated that Al/Fe-pillared palm shell activated carbon effectively removed synthetic dyes, achieving a maximum adsorption efficiency of approximately 68.89% at the fourth adsorption cycle. The adsorption performance gradually declined after subsequent reuse cycles due to pore saturation, surface fouling, and partial desorption of dye molecules.

FTIR analysis confirmed the presence of active functional groups such as –OH, –COOH, and M–O–Fe/Al, which supported both physical and chemical adsorption mechanisms. Kinetic analysis revealed that the adsorption process followed a first-order reaction, indicating that the rate depended on the dye concentration and the number of available active sites.

To maintain efficiency and extend the adsorbent lifespan, periodic regeneration using thermal or chemical methods is recommended after four reuse cycles. Future studies should focus on optimizing the regeneration process and evaluating the reusability of spent adsorbents for sustainable wastewater treatment applications.

## ACKNOWLEDGEMENTS

We would like to thank the Ministry of Education, Culture, Research, and Technology of the Republic of Indonesia for the funding provided through the Beginner Lecturer Research scheme for the 2025 fiscal year (Contract No: 123/C3/DT.05.00.PL/2025 and 077/LL2/DT.05.00/PL/2025).

## REFERENCES

Akhtar, M. S., Ali, S., & Zaman, W. (2024). Innovative Adsorbents for Pollutant Removal: Exploring the Latest Research and Applications. In *Molecules* (Vol. 29, Issue 18). Multidisciplinary Digital Publishing Institute (MDPI). https://doi.org/10.3390/molecules29184317

Alharbi, H. A., Hameed, B. H., Alotaibi, K. D., Al-Oud, S. S., & Al-Modaihsh, A. S. (2022). Recent methods in the production of activated carbon from date palm residues for the adsorption of textile dyes: A review. In *Frontiers in Environmental Science* (Vol. 10). Frontiers Media S.A. https://doi.org/10.3389/fenvs.2022.996953

Ali, R., Aslam, Z., Shawabkeh, R. A., Asghar, A., & Hussein, I. A. (2020). BET, FTIR, and RAMAN characterizations of activated carbon from waste oil fly ash. *Turkish Journal of Chemistry*, *44*(2), 279–295. https://doi.org/10.3906/KIM-1909-20

Baskar, A. V., Bolan, N., Hoang, S. A., Sooriyakumar, P., Kumar, M., Singh, L., Jasemizad, T., Padhye, L. P., Singh, G., Vinu, A., Sarkar, B., Kirkham, M. B., Rinklebe, J., Wang, S., Wang, H., Balasubramanian, R., & Siddique, K. H. M. (2022a). Recovery, regeneration and sustainable management of spent adsorbents from wastewater treatment streams: A review. In *Science of the Total Environment* (Vol. 822). Elsevier B.V. https://doi.org/10.1016/j.scitotenv.2022.153555

Baskar, A. V., Bolan, N., Hoang, S. A., Sooriyakumar, P., Kumar, M., Singh, L., Jasemizad, T., Padhye, L. P., Singh, G., Vinu, A., Sarkar, B., Kirkham, M. B., Rinklebe, J., Wang, S., Wang, H., Balasubramanian, R., & Siddique, K. H. M. (2022b). Recovery, regeneration and sustainable management of spent

adsorbents from wastewater treatment streams: A review. In *Science of the Total Environment* (Vol. 822). Elsevier B.V. https://doi.org/10.1016/j.scitotenv.2022.153555

Bumajdad, A., Khan, M. J. H., & Lukaszewicz, J. P. (2023). Nitrogen-enriched activated carbon derived from plant biomasses: a review on reaction mechanism and applications in wastewater treatment. In *Frontiers in Materials* (Vol. 10). Frontiers Media SA. https://doi.org/10.3389/fmats.2023.1218028

Dittmann, D., Saal, L., Zietzschmann, F., Mai, M., Altmann, K., Al-Sabbagh, D., Schumann, P., Ruhl, A. S., Jekel, M., & Braun, U. (2022). Characterization of activated carbons for water treatment using TGA-FTIR for analysis of oxygen-containing functional groups. *Applied Water Science*, *12*(8). https://doi.org/10.1007/s13201-022-01723-2

Jawad, A. H., Abdulhameed, A. S., Bahrudin, N. N., Hum, N. N. M. F., Surip, S. N., Syed-Hassan, S. S. A., Yousif, E., & Sabar, S. (2021). Microporous activated carbon developed from KOH activated biomass waste: surface mechanistic study of methylene blue dye adsorption. *Water Science and Technology*, *84*(8), 1858–1872. https://doi.org/10.2166/wst.2021.355

Kordijazi, A. (2021). *Applying a ssssssStatistical Approach to Develop a Sustainable Applying a Statistical Approach to Develop a Sustainable Technology for Capturing Phosphorous from an Agricultural Tile Technology for Capturing Phosphorous from an Agricultural Tile Drainage System Using By-Product Phosphorous Sorbing Drainage System Using By-Product Phosphorous Sorbing Materials (PSM) Materials (PSM)*. https://dc.uwm.edu/etd/2682

Le, T. P., Luong, H. V. T., Nguyen, H. N., Pham, T. K. T., Trinh Le, T. L., Tran, T. B. Q., & Ngo, T. N. M. (2024). Insight into adsorption-desorption of methylene blue in water using zeolite NaY: Kinetic, isotherm and thermodynamic approaches. *Results in Surfaces and Interfaces*, *16*. https://doi.org/10.1016/j.rsurfi.2024.100281

Mechnou, I., Benabdallah, A., Chham, A. I., Rachdi, Y., Hlaibi, M., El kartouti, A., & Saleh, N. (2025). Activated carbons for effective pharmaceutical adsorption: Impact of feedstock origin, activation agents, adsorption conditions, and cost analysis. In *Results in Engineering* (Vol. 27). Elsevier B.V. https://doi.org/10.1016/j.rineng.2025.105966

Peres, C. B., Morais, L. C. de, & Resende, P. M. R. (2024). Carbon adsorption on waste biomass of passion fruit peel: A promising machine learning model for CO2 capture. *Journal of CO2 Utilization*, *80*. https://doi.org/10.1016/j.jcou.2024.102680

Reddy, Y. S., Jose, T. J., Dinesh, B., Kumar, R. N., Kumar, P. S., & Kaviyarasu, K. (2025). Equilibrium, kinetic, and thermodynamic study of Direct Yellow 12 dye adsorption by biomass-derived porous graphitic activated carbon. *Biomass Conversion and Biorefinery*, *15*(5), 6817–6833. https://doi.org/10.1007/s13399-024-05464-x

Thamer, B. M., Al-aizari, F. A., & Abdo, H. S. (2023). Enhanced Adsorption of Textile Dyes by a Novel

Sulfonated Activated Carbon Derived from Pomegranate Peel Waste: Isotherm, Kinetic and Thermodynamic Study. *Molecules*, *28*(23). https://doi.org/10.3390/molecules28237712

Ullah, N., Ali, Z., Khan, A. S., Adalat, B., Nasrullah, A., & Khan, S. B. (2024). Preparation and dye adsorption properties of activated carbon/clay/sodium alginate composite hydrogel membranes. *RSC Advances*, *14*(1), 211–221. https://doi.org/10.1039/d3ra07554k